nature plants

Brief Communication

https://doi.org/10.1038/s41477-024-01850-5

Regional fire–greening positive feedback loops in Alaskan Arctic tundra

Received: 15 April 2021

Accepted: 16 October 2024

Published online: 08 November 2024

Check for updates

Dong Chen[1], Cheng Fu[2,3,4], Liza K. Jenkins[5], Jiaying He[6], Zhihao Wang[1], Randi R. Jandt[7], Gerald V. Frost[8], Allison Bredder[1], Logan T. Berner[9] & Tatiana V. Loboda[1]

Arctic tundra has experienced rapid warming, outpacing global averages, leading to significant greening whose primary drivers include widespread shrubification. Here we confirm that a fire–greening positive feedback loop is evident across the Alaskan tundra, and evidence suggests that this feedback loop is dominated by the fire–shrub interactions. We show that tundra wildfires, especially those with higher severity, play a critical role in boosting the overall greening of the tundra, often by enhancing upright deciduous shrub growth or establishment but sometimes by inducing increases in other vascular biomass. In addition, fire–greening interactions vary greatly within different tundra subregions, a likely consequence of the spatial heterogeneity in vegetation composition, climatic and geophysical conditions.

The circumpolar Arctic tundra experienced the highest rate of warming on land, with a magnitude of nearly three times the global average[1]. Rapid warming has led to extensive changes in Arctic tundra, including a widespread increase in vegetation biomass, termed 'greening'[2]. A primary driver of Arctic greening is shrubification, which includes increases in the abundance, cover and biomass of tall deciduous shrubs[3–5]. Field studies[3,6] and satellite observations[2,7] indicate that shrubification is underway across the circumpolar tundra, which has implications for the carbon cycle, energy budget and other ecosystem properties[8–11]. It is thus crucial to understand the factors that affect shrubification in the context of climate change, including wildfires.

Wildfire is an important tundra disturbance that is capable of causing substantial climatic (for example, boosting the releases of greenhouse gases[12] and lowering surface albedo[13]) and ecological (for example, affecting soil microbial composition and, thus, vegetation dynamics[14]) impacts. Palaeorecords show that tundra fires were more frequent at points in the past two millennia, which may have been fuelled by the higher dominance of deciduous shrubs[15]. Given such historical data and recent Arctic warming and shrubification, present-day tundra may be approaching a tipping point where fire activity may intensify[16,17]. There is mounting evidence for a positive feedback loop between deciduous shrubs and wildfires in the Alaskan Arctic[18–20]. Fires can lead to increased shrub cover and biomass compared with unburned sites by creating favourable conditions for shrub establishment and growth, including increased mineral soil exposure[6], improved drainage[21], higher nutrient availability[22,23] and deeper active layers[6]. Resulting deciduous shrub communities represent a more complex fuel matrix due to their substantially higher biomass and woodiness compared to tundra herbaceous and non-vascular plants. As such, they support longer residence time for flaming fires as well as residual smouldering burning[24,25]. A larger deciduous shrub fraction in vegetation composition is, therefore, likely to lead to more spatially extensive and deeper burns[18,24], forming a positive feedback loop. The existence of this fire–shrub positive feedback loop has been shown in several local-scale studies[19,20], but it is unclear whether this feedback loop operates more widely across the Alaskan tundra. Thus,

[1]Department of Geographical Sciences, University of Maryland, College Park, MD, USA. [2]College of Information and Electrical Engineering, China Agricultural University, Beijing, China. [3]Key Laboratory of Agricultural Machinery Monitoring and Big Data Applications, Ministry of Agriculture and Rural Affairs, Beijing, China. [4]Department of Geography, University of Zurich, Zurich, Switzerland. [5]Michigan Tech Research Institute, Michigan Technological University, Ann Arbor, MI, USA. [6]State Key Laboratory of Resources and Environmental Information System, Institute of Geographic Sciences and Natural Resources Research, Chinese Academy of Sciences, Beijing, China. [7]Alaska Fire Science Consortium, University of Alaska, Fairbanks, AK, USA. [8]Alaska Biological Research, Inc., Fairbanks, AK, USA. [9]School of Informatics, Computing and Cyber Systems, Northern Arizona University, Flagstaff, AZ, USA. e-mail: itscd@umd.edu

our understanding of the present-day ecosystem-wide fire regimes and our ability to develop future projections are strongly linked to our understanding of the tundra-wide patterns of the fire–shrub relationship beyond local-scale observations.

In this study, we examined the relationship between wildfires and tundra vegetation succession across the Alaskan Arctic using four decades of Landsat satellite observations and field data. Specifically, we quantified changes in tundra greenness using the annual maximum normalized difference vegetation index ($NDVI_{max}$), which tends to positively correlate with deciduous shrub growth and aboveground biomass[2,26]. We focused on four tundra subregions that span gradients of climate, permafrost conditions and wildfire regime in Arctic Alaska: the Noatak River Valley (hereafter referred to as Noatak), the Seward Peninsula (Seward), the North Slope and the Southwest (Extended Data Fig. 1). We quantified $NDVI_{max}$ anomaly trajectories for burned areas across the four subregions using Landsat data from a large random sample of points located within and adjacent to historical wildfire perimeters (Extended Data Fig. 2). In all four tundra subregions, we found that $NDVI_{max}$ was generally higher several decades after wildfire compared with unburned tundra, particularly at sites that experienced high-severity burns (Fig. 1). In high-severity burns, the initial decrease in $NDVI_{max}$, associated with consumption of aboveground biomass and deposition of char and ash on the surface, tended to dissipate within the first five years after fire. Beyond the first five years, the post-fire $NDVI_{max}$ of severe burns exceeded that of unburned control sites, showing a statistically significant difference throughout our tracking period of ~30 years after a fire event ($\alpha = 0.01$, t-test). In Seward, however, the apparent increases in $NDVI_{max}$ anomaly were not statistically significant (Fig. 1). In contrast with high-severity burns, sites with low-severity burns exhibited limited changes in post-fire $NDVI_{max}$ compared with unburned tundra. Except for the initial post-fire periods in the North Slope and Noatak, the $NDVI_{max}$ of low-severity burns was practically indistinguishable from that of the unburned tundra. As expected, moderate-severity burns show post-fire $NDVI_{max}$ patterns that are intermediate.

Our analysis also revealed that the pre-fire $NDVI_{max}$ of most high-severity burns was notably higher than that of unburned tundra in all four subregions (Fig. 1). This indicates that the severity of a fire event is linked to the pre-fire vegetation conditions, potentially the fuel load. The $NDVI_{max}$ patterns shown during the pre- and post-fire stages, taken together, indicate that a fire–greening positive feedback loop may exist in at least three of the four subregions of the Alaskan tundra, excluding Seward. Burn severity is driven by pre-fire biomass (greenness) and drives its magnitude post-fire, completing the fire–greening positive feedback loop.

Deciduous shrub growth and abundance have been found to be strongly correlated with NDVI by previous studies[27,28], although low correlations have also been previously reported at local scales[29]. In addition, NDVI can reflect the presence of graminoids[2], which also play an important role in tundra ecosystems and are usually the dominant vegetation type during the early recovery stage of post-fire tundra sites[30,31]. To better understand the relative contributions of plant functional types (PFTs) to greening in our study area, we examined correlations between $NDVI_{max}$ and tundra vegetation cover across the Alaskan tundra by comparing Landsat $NDVI_{max}$ with field measurements of fractional deciduous shrub, evergreen shrub and graminoid cover from the Alaska Vegetation Plots Database (AKVEG)[32], which is the largest collection of in situ species-level vegetation cover data across the Alaskan tundra that we are aware of (Extended Data Fig. 3). The results (Extended Data Fig. 4) showed that $NDVI_{max}$ is almost always significantly ($P < 0.01$) and positively correlated with deciduous shrub cover, but generally not significantly ($P < 0.01$) correlated with evergreen shrub cover and graminoid cover at the regional level.

Our hypothesis that deciduous shrubs are one of the dominant drivers of the fire–greening positive feedback loop is further supported by field data that we collected over a 3-year period (2016–2018) across a chronosequence of burns in Noatak and Seward tundra. The goal was to assess post-fire vegetation succession during the first five decades using a space-for-time substitution approach; thus, we collected detailed measurements of vegetation composition across a large number of burns of different ages. The dataset includes assessments of shrub fractional cover, shrub species, stem count and stem diameter measurements on 1 m × 1 m plots. We found in both Noatak and Seward that post-fire tundra had higher shrub cover than the unburned sites (Fig. 2a), albeit with different magnitudes and durations, as discussed in the following section. Field data indicated that shrub dynamics in both regions were driven by deciduous shrub species, specifically dwarf birch (*Betula nana*) in Noatak and willows (*Salix* spp.) in Seward (Extended Data Fig. 5). Overall, both our field and remote-sensing analyses suggest an increased abundance of deciduous shrubs several decades after fire, which is probably an important aspect of the fire–greening feedback loop.

Even though post-fire greening was evident across the Alaskan tundra as a whole, we found that the magnitude of the effect varied substantially both within and among subregions. The most notable difference in the fire–greening relationship was between Noatak and Seward, the two tundra subregions with very active recent histories of burning[33] and of similar erect-shrub tundra physiognomic type (according to the Circumpolar Arctic Vegetation Map[34] (CAVM)). In Noatak, at the majority of burned sites, the post-fire $NDVI_{max}$ was significantly higher than that of unburned control sites within several years of burning (Fig. 1). Higher $NDVI_{max}$ lasted for several decades until the end of the study period. In contrast, the Seward region high-severity burned sites did not show a statistically significant increase in post-fire $NDVI_{max}$ (Fig. 1), in any of the three main physiognomic types (that is, erect-shrub tundra, graminoid tundra and wetland; Extended Data Fig. 6). Except for a few years immediately after fire, the post-fire $NDVI_{max}$ of Seward burn scars was practically indistinguishable from that of unburned sites.

Our Noatak and Seward field data provided unique insights into this NDVI disparity. We found that, in Noatak, shrub biomass increased steadily after fires, whereas, in Seward, shrub biomass experienced a minor increase in the second decade after the fires then decreased to the unburned level by the fifth decade (Fig. 2b). In addition, in Noatak, shrub biomass initially recovers through rapid reestablishment of shrubs, co-dominated by dwarf birch and bog Labrador tea (*Rhododendron groenlandicum*) (Extended Data Fig. 7a). As the shrubs mature, in the second decade, the total number of individual stems decreases, but their diameter, shrub height and shrub cover continue to grow (not shown) with the overall dominance of dwarf birch (*Betula nana*) (Extended Data Fig. 7a). Bog Labrador tea and willow appeared to wane slowly as dwarf birch increased and, by the fifth decade, had almost disappeared at the burned sites that we visited (Extended Data Fig. 7a). In Seward, we observed a nearly identical pre-fire shrub biomass (Fig. 2b) but a different post-fire trajectory that results in no discernable increase in shrub cover, shrub height and total biomass over time (not shown). Although *Betula* shrubs are present, in Seward, shrub biomass is dominated by willows (*Salix* spp.), whose biomass increases almost continuously with stand age (Extended Data Fig. 7b). Our fine-scale plot data thus suggest that the divergent post-fire shrub pathways observed in the two subregions may be at least partly driven by pre-existing differences in PFT and shrub species dominance.

Tundra wildfires have received less attention from the scientific community and general public because of their relative infrequency and low direct impacts on human populations. However, the expected increases in fire extent, frequency and severity[16,35], coupled with the crucial role of circumpolar tundra in global climate change, render understanding tundra fires an urgent and strategically important matter. Previous studies documented a local-scale fire–shrub positive feedback loop in the tundra[19,20]. Our results, by linking field-measured

https://doi.org/10.1038/s41477-024-01850-5

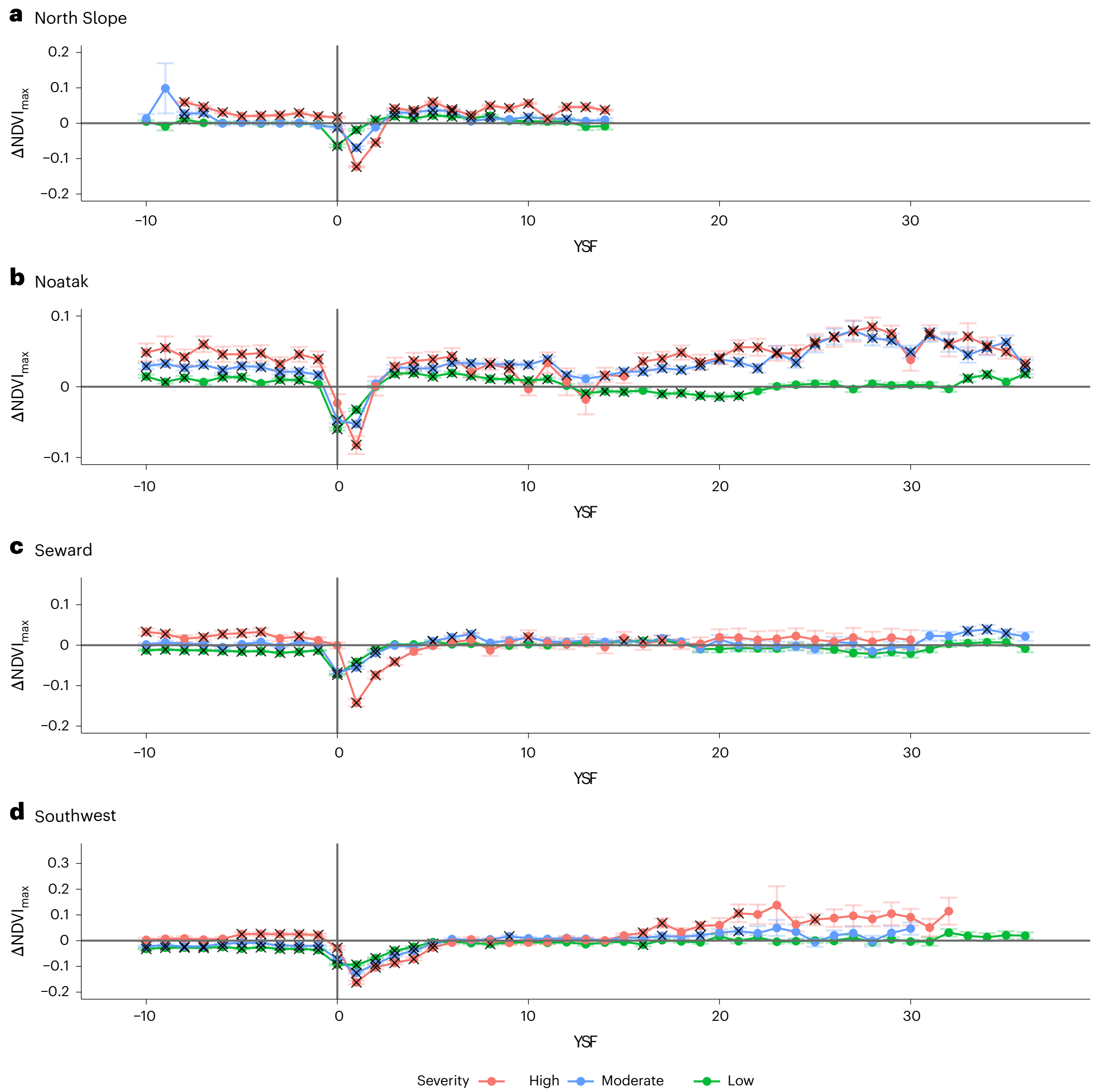

Fig. 1 | The post-fire $NDVI_{max}$ anomaly trajectories generated using Landsat data. a–d, The trajectories were calculated based on sample points from the North Slope (**a**), Noatak (**b**), Seward (**c**) and the Southwest (**d**). The points marked by crosses represent the YSF values when the $NDVI_{max}$ of the burned sites was statistically different from that of the unburned sites on the basis of paired two-tailed *t*-tests ($P < 0.01$). The error bars denote ±1 standard error, with the centres being the mean $NDVI_{max}$ anomaly values. The sample size for each point, as well as the *P* values from the *t*-tests, are provided in Supplementary Table 1.

shrub presence with NDVI, indicate that this phenomenon exists at a regional scale across the Alaskan tundra. In addition, we show that tundra wildfires, especially those with higher severity, often lead to long-term increases in tundra greenness and deciduous shrub dominance, which, in turn, provide higher fuel loads and could increase the probability of subsequent severe fires. This has important implications for climate change. Under current Arctic warming, much of the Arctic tundra biome is experiencing substantial greening and shrubs are a major contributor to this process[2,36]. Even though both warming and wildfire have been suggested to boost shrubification, our results show that during the 21-year period between 2001 and 2021, the increases in $NDVI_{max}$ at the high-severity burned sites (indicated by the red lines in Extended Data Fig. 8) are often similar to or larger than the mean $NDVI_{max}$ differences as observed between the high-severity burned sites and the background sites (indicated by the blue lines in Extended Data Fig. 8) (except in Noatak, where no statistically significant increasing trends were identified in either burned and background sites). This means that, at least in recent decades, high-severity fires may have promoted the shrubification process at a magnitude that is on par with that of the warming-induced shrubification, allowing severely burned sites to green up much faster than the background greening rate that was already substantial. Considering future projections of increases in wildfire occurrence, extent and severity in the high northern latitudes[17,35], the strong boosting effect of high-severity fires on shrubification as we have shown is likely to translate into substantial impacts on the species composition and successional trajectory of tundra ecosystems towards an accelerated shrubification of this biome. Our findings also underscore the heterogeneity in wildfire–vegetation interactions throughout the Alaskan tundra. This, combined with our limited comprehension of wildfires' impacts on tundra ecosystems compared with those in other biomes, necessitates intensified and systematic data synthesis and acquisition efforts. Recently, there have been several projects, including the Synthesized Alaskan Tundra Field Database[37], that synthesized existing field data collected in the Arctic tundra. Additional efforts should encompass field campaigns and remote-sensing data acquisitions conducted systematically across the

 https://doi.org/10.1038/s41477-024-01850-5

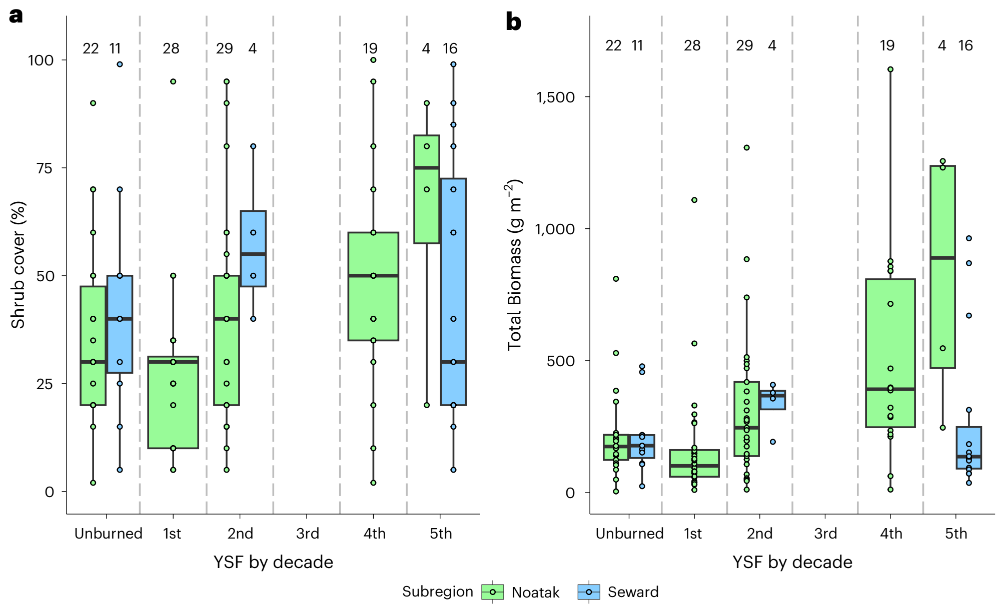

Fig. 2 | Boxplots generated based on field data. a,**b**, They show the relationship between YSF and per cent shrub cover (**a**) and total shrub biomass (g m^{-2}) (**b**), as measured in our field plots. Each circle indicates an observation, with the total number of plots (*n*) at the top of each column. Within each boxplot, the upper and lower ends of the box represent the upper and lower quartiles, respectively. The centre of the box denotes the median value, while the whiskers extend 1.5 times the interquartile range above the upper quartile and below the lower quartile, respectively.

Arctic tundra allowing us to monitor fire–vegetation dynamics across different tundra gradients.

Methods

$NDVI_{max}$ versus fractional cover of shrubs and graminoids

Our primary aim is to confirm that the common satellite-based observation of vegetation greenness ($NDVI_{max}$) is representative of vegetation composition in relation to deciduous shrub cover in the Alaskan tundra and can be used reliably to assess ecosystem-wide changes and make inferences about vegetation composition. We adopted the AKVEG[32], which, to our knowledge, is the largest field database that contains species-level vegetation cover data for Alaska. We extracted the vegetation cover data for all field sites (which are 12.5-m-radius circles, following the field data collection protocol[38] developed by the Vegetation Working Group of the Alaska Geospatial Council) across the Alaskan tundra (Extended Data Fig. 3), and for each site, we grouped the vegetation cover values from all plants into a few PFTs, including evergreen shrub, deciduous shrub and graminoid. $NDVI_{max}$ for each field plot of the newly compiled dataset was then extracted on Google Earth Engine (GEE) based on the Landsat surface reflectance data for June–August in the corresponding year. For example, $NDVI_{max}$ for 2012 was extracted for field plot A if the in situ data at field plot A were collected in 2012. $NDVI_{max}$ and observed (according to AKVEG) shrub and graminoid cover for all four subregions were compared using simple linear regression (Extended Data Fig. 4).

Extraction of $NDVI_{max}$ and $NDVI_{max}$ anomaly trajectories

For our domain-wide analysis, annual $NDVI_{max}$ time series were produced for randomly generated sample points across the Alaskan tundra. Three types of random sample points—burned, unburned and background—were created. Burned sample points were generated within areas that have experienced burning between 1985 and 2017 as reported by the Monitoring Trends in Burn Severity (MTBS) product[39]. We adopted MTBS because it provides not only human-guided identification of burned areas within burn scars that are larger than 400 ha in Alaska, but also the burn severity levels (that is, low, moderate and high) of burn areas within the scars. It is worth noting that the severity levels provided by MTBS are somewhat subjective as the severity level thresholds were determined by analysts visually[39]. While this inevitably introduces uncertainties, we still chose MTBS because (1) it is the only large-scale burn severity dataset that is consistently produced and covers our study area, and (2) it adopts a series of quality-control measures, including cross-calibration among a team of interpreters and thresholding based on not just differenced normalized burn ratio (dNBR) but also 'relativized' dNBR (RdNBR[40]) as well as pre- and post-fire satellite imagery[39].

Areas that experienced more than one fire during 1985–2017 were excluded to minimize the compounding effect that repeated burns may have on the post-fire vegetation recovery. Unburned sample points were generated within the buffered zone (determined as the areas between two buffer distances—50 m and 1,000 m—from each burn scar) of the burn scars. Each unburned point was matched to a burned point from the same burn scar (to allow for $NDVI_{max}$ anomaly calculation). Background sample points were generated within the areas across the four tundra subregions that are below 300 m above sea level (our previous unpublished results showed that less than 7% of burned areas since the 1940s in Alaskan tundra occurred above the 300 m line). For each burned point, an unburned point (from the same burn scar) and a background point were matched, resulting in a three-point trio. Overall, we generated 5,000 trios for each subregion, leading to a total of 60,000 sample points for the entire Alaskan tundra (shown in Extended Data Fig. 2).

Before being used to extract $NDVI_{max}$ on GEE, the random sample points were checked against a water mask produced on the basis of the 30 m Global Surface Water dataset[41]. To minimize the negative influence of water on NDVI calculation, we intentionally created a very liberal water mask. To that end, we buffered all water pixels with >50% of water occurrence as identified by Global Surface Water for 90 m (three Landsat pixels). If any one of the three sample points of the same trio was found to overlap with the water mask, the entire trio was excluded from subsequent analyses. The remaining sample points were used to estimate annual $NDVI_{max}$ based on all Landsat 5, 7 and 8 surface reflectance data collected during the summer between 1985 and 2021. The sensors on these Landsat satellites have different spectral properties[2]; therefore, we calibrated surface reflectance data from Landsat 5 and Landsat 8 to Landsat 7 using a machine learning algorithm in the LandsatTS package for R[42], after which we estimated annual $NDVI_{max}$ based on a phenological modelling approach also implemented in LandsatTS.

The $NDVI_{max}$ data included more than 1 million unique $NDVI_{max}$ retrievals and were subjected to two analyses. The first analysis centred on the establishment of the $NDVI_{max}$ anomaly trajectories. Specifically, for each burned sample point, its $NDVI_{max}$ anomaly for a given year (that is, any year between 1985 and 2021) was calculated by subtracting the $NDVI_{max}$ value of its matched unburned point for the same year from its $NDVI_{max}$ value. For example, if the $NDVI_{max}$ values of burned sample point A and its matched unburned sample point B for the year 1985 were 0.622 and 0.543, respectively, the $NDVI_{max}$ anomaly value for point A in 1985 was 0.079. An $NDVI_{max}$ anomaly trajectory was created for each subregion by calculating and plotting the average $NDVI_{max}$ anomaly values of the burned points for each year since fire (YSF) value, calculated as $Year_{observation} - Year_{fire}$. We considered burn severity, landscape and physiognomic types in the trajectory establishment. Specifically, burned samples were grouped by burn severity level (that is, high, moderate and low, as indicated by the MTBS dataset), landscape types (that is, upland and lowland, according to Muller, et al.[43]; Extended Data Fig. 7) and physiognomic types (that is, graminoid tundra, erect-shrub tundra and wetland, as indicated by the 1 km CAVM raster dataset[44]) and calculated $NDVI_{max}$ anomalies separately for each of the categories.

The second analysis compared post-fire increases in greenness against background warming-induced greening across the tundra over the past decades. We located all burned sample points that experienced burning between 1985 and 2000 (according to MTBS) and calculated their $NDVI_{max}$ trajectories during 2006–2020. A 5-year gap between 2001 and 2005 was implemented intentionally because our $NDVI_{max}$ anomaly trajectories showed that most post-fire decreases in $NDVI_{max}$ tend to disappear within 5 years. We also calculated the 2006–2020 $NDVI_{max}$ trajectories of unburned and background sample points paired with each burn point. These trajectories were plotted together to highlight their similarities and differences.

Field data collection

We conducted field measurements during three field campaigns to the Alaskan tundra between July and August of 2016–2018, with two visits to Noatak and one visit to Seward. The field sites were identified before our field trips on the basis of a stratified randomized scheme taking into account a combination of factors including drainage (calculated on the basis of the US Geological Survey interferometric synthetic aperture radar digital elevation model data) and year since the last fire (calculated on the basis of the Alaska Large Fire Database[45]). A surplus of potential field sites was generated during the planning stage, and it was up to the field team to determine which sites to visit based on the time limit and accessibility of the sites when they were in the tundra. The field team also decided the locations of the unburned sites, that is, sites that shared similar surface conditions as the burned sites but had not experienced known fires. Eventually, a total of 137 sites (Noatak: 83 burned + 22 unburned; Seward: 21 burned + 11 unburned) that were confirmed to have burned only once since the 1970s were visited during the three campaigns. At each site, the field team conducted measurements for a series of vegetation-related parameters at a 1 m × 1 m plot within which we estimated the shrub cover and counted the number of shrub species as well as the number of stems of each species. We also estimated the biomass of the shrubs found within the 1 m × 1 m plot by applying the allometric equations developed by Smith and Brand[46] that relate basal diameters to biomass. In addition, mean shrub height and per cent shrub cover were measured and estimated, respectively.

Reporting summary

Further information on research design is available in the Nature Portfolio Reporting Summary linked to this article.

Data availability

All data used in this paper are publicly accessible. The field data that our team collected are available through the Oak Ridge National Laboratory Distributed Active Archive Center (ORNL DAAC) at https://doi.org/10.3334/ORNLDAAC/1919. The AKVEG is available at https://akveg.uaa.alaska.edu/. The MTBS product is available at https://www.mtbs.gov/. The CAVM dataset is available at https://www.geobotany.uaf.edu/cavm/. The LandsatTS package for R is available via GitHub at https://github.com/logan-berner/LandsatTS. Visualizations in this paper were implemented using ArcGIS Desktop (v10.6), and R (v3.5.1). Data analyses were carried out using R (v3.5.1), Python (v2.7.14), IDL (v8.5) and GEE.

References

1. *Arctic Climate Change Update 2021: Key Trends and Impacts. Summary for Policy-Makers* 16 (AMAP, 2021).
2. Berner, L. T. et al. Summer warming explains widespread but not uniform greening in the Arctic tundra biome. *Nat. Commun.* **11**, 4621 (2020).
3. Elmendorf, S. C. et al. Plot-scale evidence of tundra vegetation change and links to recent summer warming. *Nat. Clim. Change* **2**, 453–457 (2012).
4. Sturm, M., Racine, C. & Tape, K. Climate change: increasing shrub abundance in the Arctic. *Nature* **411**, 546–547 (2001).
5. Mekonnen, Z. A. et al. Arctic tundra shrubification: a review of mechanisms and impacts on ecosystem carbon balance. *Environ. Res. Lett.* **16**, 053001 (2021).
6. Myers-Smith, I. H. et al. Shrub expansion in tundra ecosystems: dynamics, impacts and research priorities. *Environ. Res. Lett.* **6**, 045509 (2011).
7. Stow, D. A. et al. Remote sensing of vegetation and land-cover change in Arctic tundra ecosystems. *Remote Sens. Environ.* **89**, 281–308 (2004).
8. Pearson, R. G. et al. Shifts in Arctic vegetation and associated feedbacks under climate change. *Nat. Clim. Change* **3**, 673–677 (2013).
9. Sistla, S. A. et al. Long-term warming restructures Arctic tundra without changing net soil carbon storage. *Nature* **497**, 615–618 (2013).
10. Blok, D. et al. Shrub expansion may reduce summer permafrost thaw in Siberian tundra. *Glob. Change Biol.* **16**, 1296–1305 (2010).
11. Loranty, M. M., Goetz, S. J. & Beck, P. S. A. Tundra vegetation effects on pan-Arctic albedo. *Environ. Res. Lett.* **6**, (2011).
12. Mack, M. C. et al. Carbon loss from an unprecedented Arctic tundra wildfire. *Nature* **475**, 489–492 (2011).
13. French, N. H. F., Whitley, M. A. & Jenkins, L. K. Fire disturbance effects on land surface albedo in Alaskan tundra. *J. Geophys. Res. Biogeosci.* **121**, 841–854 (2016).
14. Hewitt, R. E., Hollingsworth, T. N., Stuart Chapin Iii, F. & Lee Taylor, D. Fire-severity effects on plant–fungal interactions after a novel tundra wildfire disturbance: implications for arctic shrub and tree migration. *BMC Ecol.* **16**, 25 (2016).
15. Higuera, P. E. et al. Frequent fires in ancient shrub tundra: implications of paleorecords for arctic environmental change. *PLoS ONE* **3**, e0001744 (2008).
16. Hu, F. S. et al. Arctic tundra fires: natural variability and responses to climate change. *Front. Ecol. Environ.* **13**, 369–377 (2015).
17. French, N. H. F. et al. Fire in arctic tundra of Alaska: past fire activity, future fire potential, and significance for land management and ecology. *Int. J. Wildland Fire* **24**, 1045–1061 (2015).
18. Higuera, P. E., Chipman, M. L., Barnes, J. L., Urban, M. A. & Hu, F. S. Variability of tundra fire regimes in Arctic Alaska: millennial-scale patterns and ecological implications. *Ecol. Appl.* **21**, 3211–3226 (2011).

19. Gaglioti, B. V. et al. Tussocks enduring or shrubs greening: alternate responses to changing fire regimes in the Noatak River Valley, Alaska. *J. Geophys. Res. Biogeosci.* **126**, e2020JG006009 (2021).
20. Chen, Y., Hu, F. S. & Lara, M. J. Divergent shrub-cover responses driven by climate, wildfire, and permafrost interactions in Arctic tundra ecosystems. *Glob. Change Biol.* **27**, 652–663 (2021).
21. Fastie, C. L., Lloyd, A. H. & Doak, P. Fire history and postfire forest development in an upland watershed of interior Alaska. *J. Geophys. Res. Atmos.* **108**, (2002).
22. Mack, M. C., Schuur, E. A. G., Bret-Harte, M. S., Shaver, G. R. & Chapin, F. S. Ecosystem carbon storage in arctic tundra reduced by long-term nutrient fertilization. *Nature* **431**, 440–443 (2004).
23. Racine, C., Jandt, R., Meyers, C. & Dennis, J. Tundra fire and vegetation change along a hillslope on the Seward Peninsula, Alaska, U.S.A. *Arct. Antarct. Alp. Res.* **36**, 1–10 (2004).
24. Higuera, P. E., Brubaker, L. B., Anderson, P. M., Hu, F. S. & Brown, T. A. Vegetation mediated the impacts of postglacial climate change on fire regimes in the south-central Brooks Range, Alaska. *Ecol. Monogr.* **79**, 201–219 (2009).
25. Bailey, A. W. & Anderson, M. L. Fire temperatures in grass, shrub and aspen forest communities of Central Alberta. *J. Range Manag. Arch.* **33**, 37–40 (1980).
26. Berner, L. T., Jantz, P., Tape, K. D. & Goetz, S. J. Tundra plant above-ground biomass and shrub dominance mapped across the North Slope of Alaska. *Environ. Res. Lett.* **13**, 035002 (2018).
27. Blok, D. et al. The response of Arctic vegetation to the summer climate: relation between shrub cover, NDVI, surface albedo and temperature. *Environ. Res. Lett.* **6**, 035502 (2011).
28. Tape, K. E. N., Sturm, M. & Racine, C. The evidence for shrub expansion in Northern Alaska and the Pan-Arctic. *Glob. Change Biol.* **12**, 686–702 (2006).
29. Cunliffe, A. M. et al. Aboveground biomass corresponds strongly with drone-derived canopy height but weakly with greenness (NDVI) in a shrub tundra landscape. *Environ. Res. Lett.* **15**, 125004 (2020).
30. Bret-Harte, M. S. et al. The response of Arctic vegetation and soils following an unusually severe tundra fire. *Philos. Trans. R. Soc. B* **368**, 20120490 (2013).
31. Racine, C. H., Johnson, L. A. & Viereck, L. A. Patterns of vegetation recovery after tundra fires in Northwestern Alaska, U.S.A. *Arct. Alp. Res.* **19**, 461–469 (1987).
32. Nawrocki, T. W. et al. Alaska Vegetation Plots (AKVEG) database. https://akveg.uaa.alaska.edu/ (University of Alaska Anchorage, 2022).
33. Rocha, A. V. et al. The footprint of Alaskan tundra fires during the past half-century: implications for surface properties and radiative forcing. *Environ. Res. Lett.* **7**, 044039 (2012).
34. Walker, D. A. et al. The Circumpolar Arctic Vegetation Map. *J. Veg. Sci.* **16**, 267–282 (2005).
35. Hu, F. S. et al. Tundra burning in Alaska: linkages to climatic change and sea ice retreat. *J. Geophys. Res. Biogeosci.* **115**, (2010).
36. Heijmans, M. M. P. D. et al. Tundra vegetation change and impacts on permafrost. *Nat. Rev. Earth Environ.* **3**, 68–84 (2022).
37. Zhu, X. et al. A synthesized field survey database of vegetation and active-layer properties for the Alaskan tundra (1972–2020). *Earth Syst. Sci. Data* **16**, 3687–3703 (2024).
38. Field data collection protocol for the Alaska Vegetation Map Version 1.0. *AGC VWG* https://agc-vegetation-soa-dnr.hub.arcgis.com/ (2024).
39. Eidenshink, J. C. et al. A project for monitoring trends in burn severity. *Fire Ecol.* **3**, 3–21 (2007).
40. Miller, J. D. & Thode, A. E. Quantifying burn severity in a heterogeneous landscape with a relative version of the delta normalized burn ratio (dNBR). *Remote Sens. Environ.* **109**, 66–80 (2007).
41. Pekel, J.-F., Cottam, A., Gorelick, N. & Belward, A. S. High-resolution mapping of global surface water and its long-term changes. *Nature* **540**, 418–422 (2016).
42. Berner, L. T., Assmann, J. J., Normand, S. & Goetz, S. J. 'LandsatTS': an R package to facilitate retrieval, cleaning, cross-calibration, and phenological modeling of Landsat time series data. *Ecography* **2023**, e06768 (2023).
43. Muller, S., Walker, D. A. & Jorgenson, M. T. Land Cover and Ecosystem Map Collection for Northern Alaska. https://doi.org/10.3334/ORNLDAAC/1359 (ORNL Distributed Active Archive Center, 2018).
44. Raynolds, M. K. et al. A raster version of the Circumpolar Arctic Vegetation Map (CAVM). *Remote Sens. Environ.* **232**, 111297 (2019).
45. Kasischke, E. S., Williams, D. & Barry, D. Analysis of the patterns of large fires in the boreal forest region of Alaska. *Int. J. Wildland Fire* **11**, 131–144 (2002).
46. Smith, W. B. & Brand, G. J. *Allometric Biomass Equations for 98 Species of Herbs, Shrubs, and Small Trees* (US Department of Agriculture, 1983).

Acknowledgements

This study was funded by NASA ABoVE and was supported by the NASA Terrestrial Ecology programme grant NNX15AT79A (T.V.L.).

Author contributions

D.C.: conceptualization, methodology, software, data curation, field work, writing – original draft, writing – review and editing, visualization and project administration. C.F.: methodology and software. L.K.J.: field work. J.H.: field work and writing – review and editing. Z.W.: methodology and software. R.R.J.: writing – review and editing. G.V.F.: writing – review and editing. A.B.: writing – original draft, and writing – review and editing. L.T.B.: writing – review and editing. T.V.L.: field work, writing – review and editing, project administration and funding acquisition.

Competing interests

The authors declare no competing interests.

Additional information

Extended data is available for this paper at https://doi.org/10.1038/s41477-024-01850-5.

Supplementary information The online version contains supplementary material available at https://doi.org/10.1038/s41477-024-01850-5.

Correspondence and requests for materials should be addressed to Dong Chen.

Peer review information *Nature Plants* thanks the anonymous reviewers for their contribution to the peer review of this work.

 https://doi.org/10.1038/s41477-024-01850-5

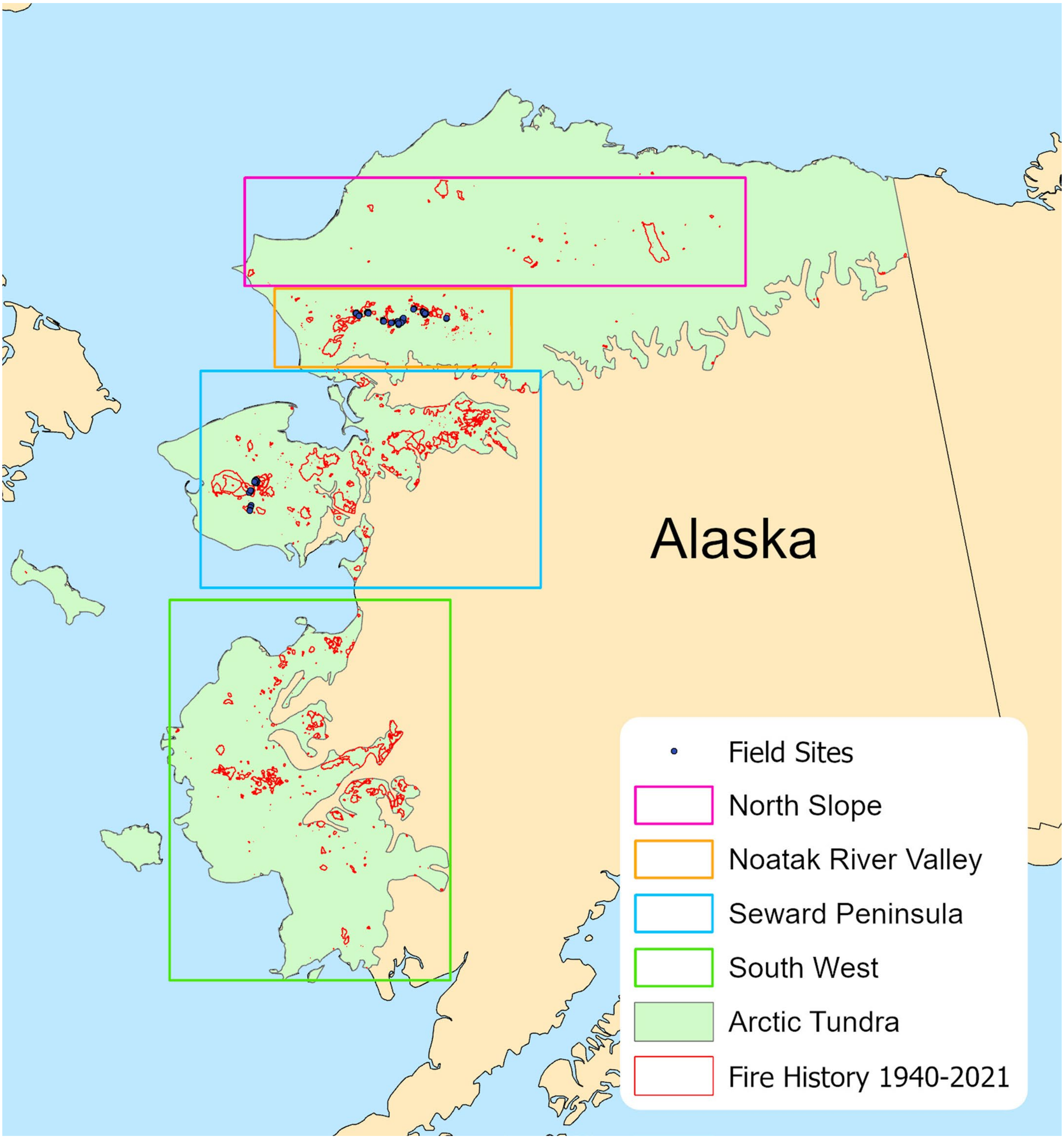

Extended Data Fig. 1 | Distribution of field sites and the four tundra subregions. The boundary of the Arctic tundra is delineated based on the Circumpolar Arctic Vegetation Map[34] (CAVM). Historical fire perimeters (red) are based on the Alaska Large Fire Database[45] from 1940 to 2021. Field data in Seward and Noatak were collected by our team, which are available at https://doi.org/10.3334/ORNLDAAC/1919.

 https://doi.org/10.1038/s41477-024-01850-5

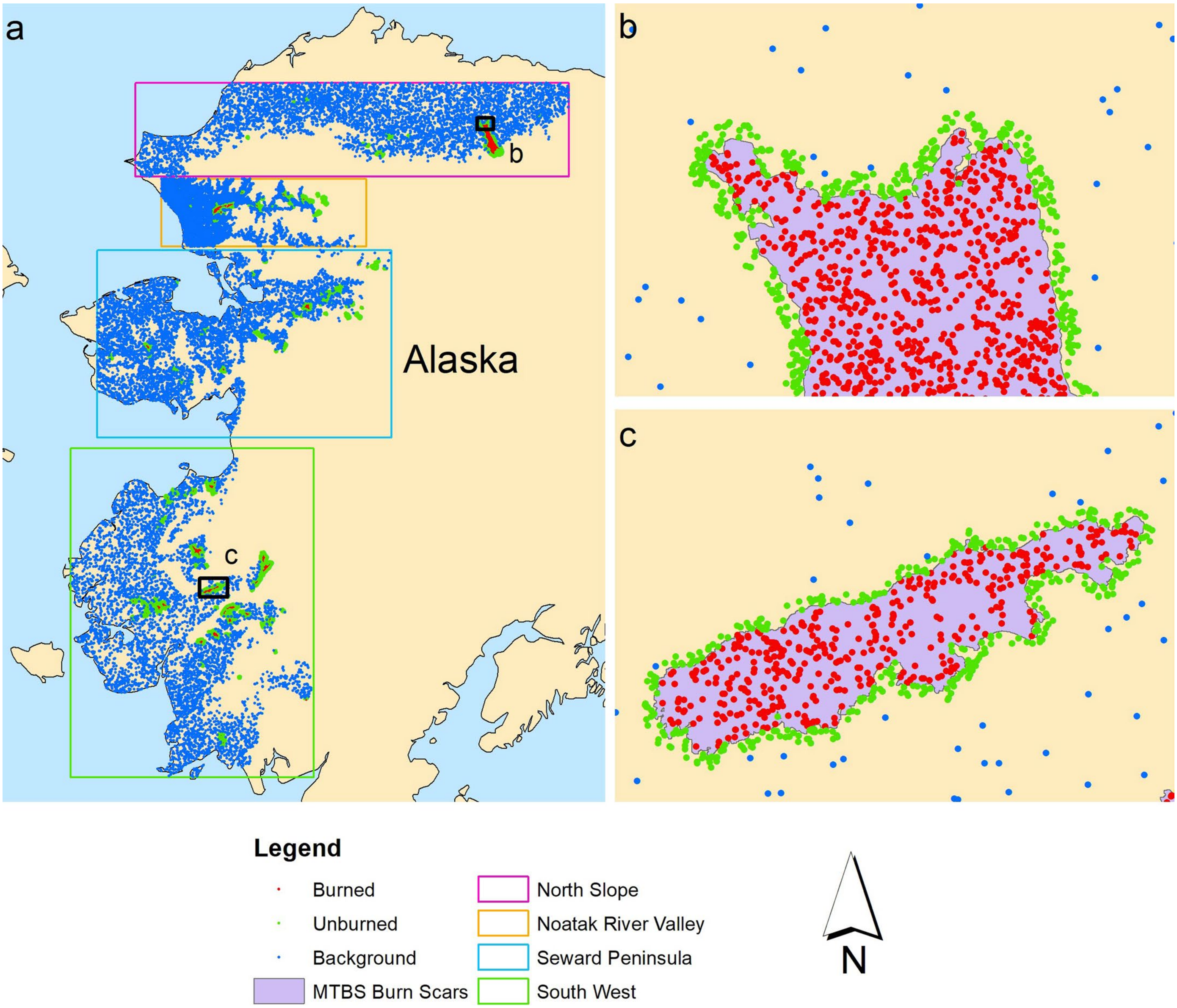

Extended Data Fig. 2 | Distribution of random sample points generated across the Alaskan tundra. Red, green, and blue points represent burned, unburned, and background sites, respectively. Panel (**a**) shows an overall view across the Alaskan tundra, while panels (**b**) and (**c**) offer close-up views of two specific locations.

https://doi.org/10.1038/s41477-024-01850-5

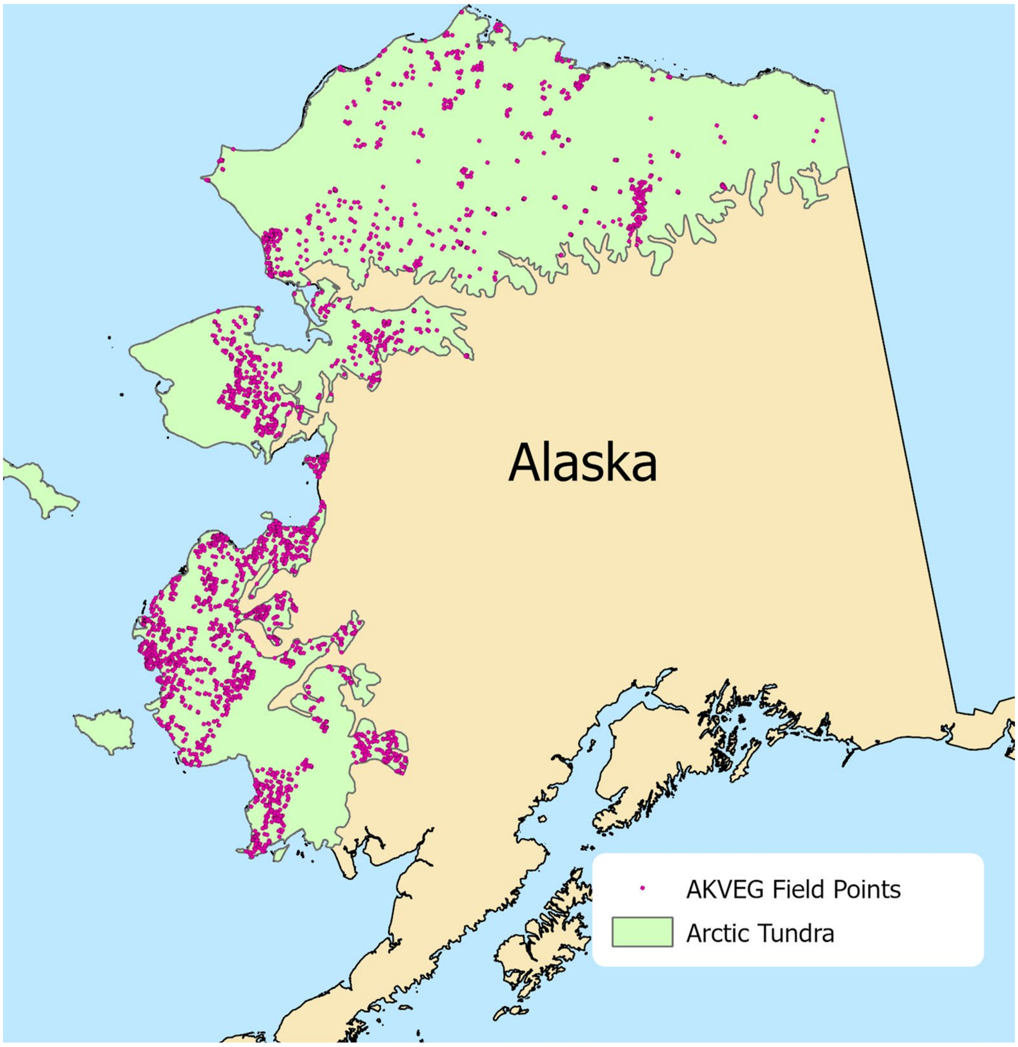

Extended Data Fig. 3 | The distribution of AKVEG field points. The distribution of the tundra field points that the Alaska Vegetation Plots Database (AKVEG)[32] contains.

 https://doi.org/10.1038/s41477-024-01850-5

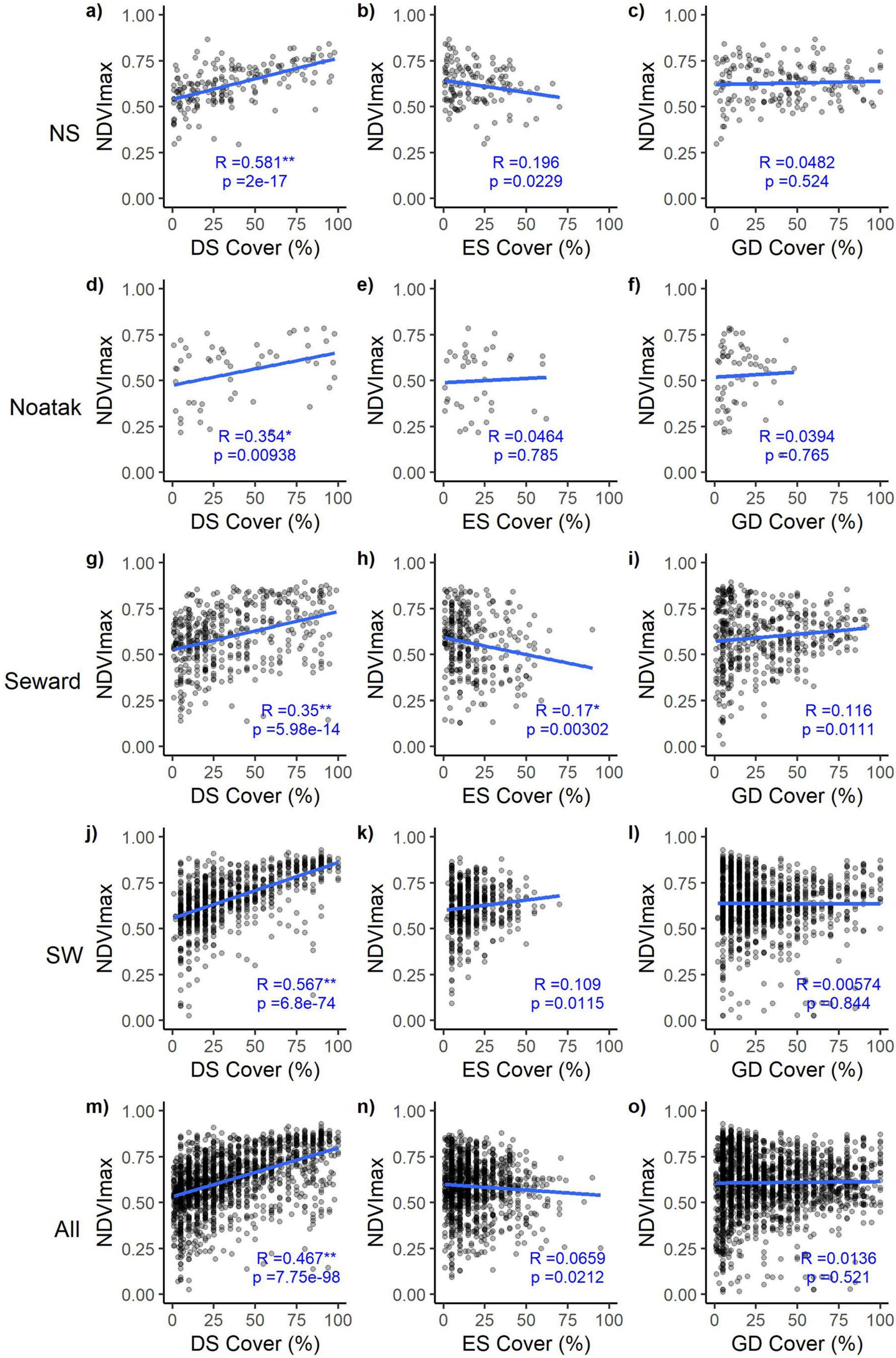

Extended Data Fig. 4 | Scatterplots of field-measured shrub and graminoid cover and NDVI$_{max}$ by years since fire based on Landsat imagery on GEE. **a**–**l**, Panels correspond to tundra subregions North Slope (**a**–**c**), Noatak (**d**–**f**), Seward (**g**–**i**), and Southwest (**j**–**l**). **m**–**o**, Panels correspond to all of the Alaskan tundra. Symbols '*' and '**' after the correlation (R) values correspond to p < 0.01 and 0.001, respectively. Field data were from AKVEG. DS: deciduous shrub; ES: evergreen shrub; GD: graminoid.

https://doi.org/10.1038/s41477-024-01850-5

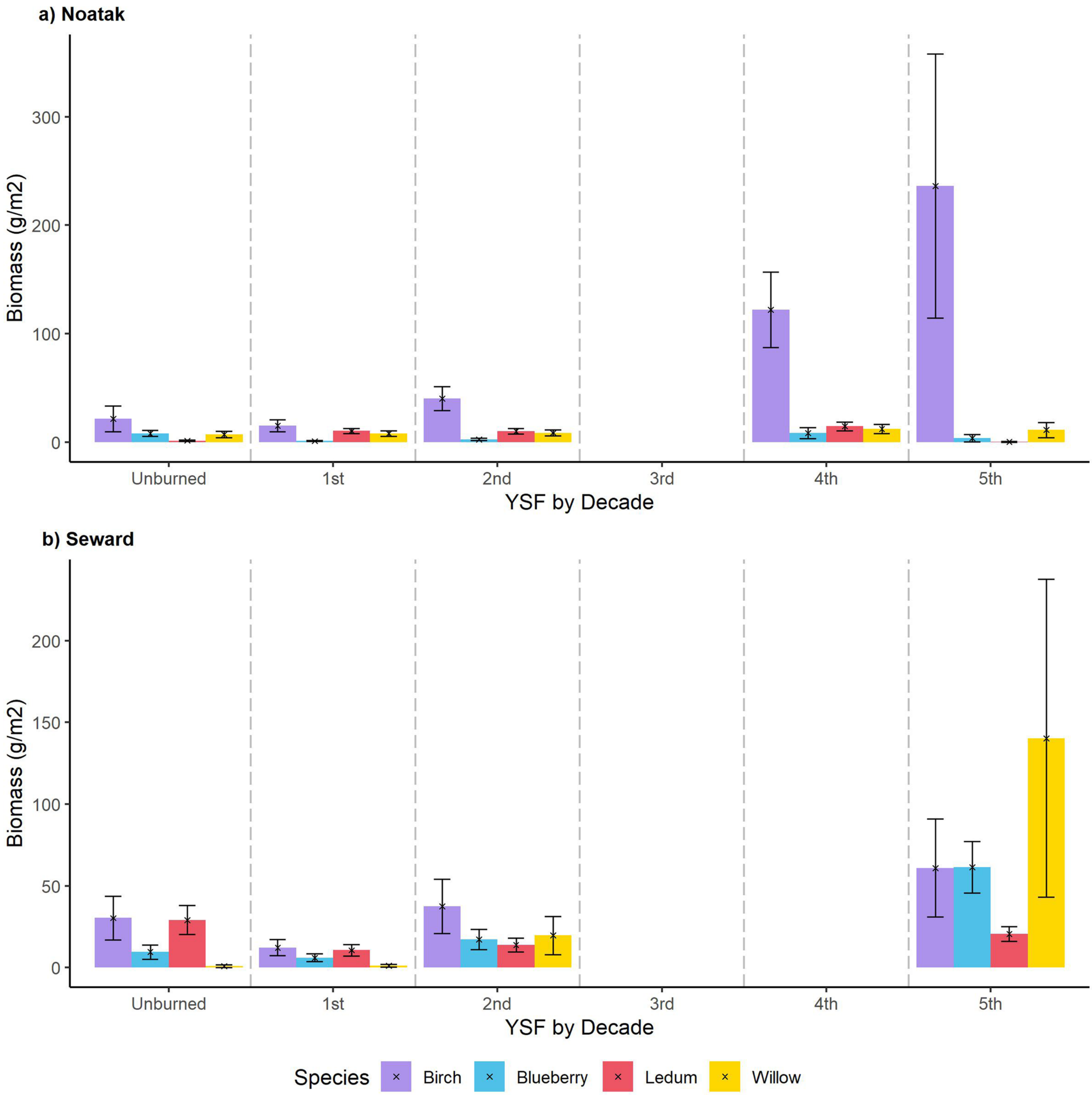

Extended Data Fig. 5 | Mean biomass of four dominant shrub species for each stand age group calculated based on 1 x 1m plots in Noatak (a) and Seward (b). YSF: year since fire. Birch: *Betula nana;* Blueberry*: Vaccinium uliginosum;* Ledum*: Rhododendron groenlandicum* (bog Labrador tea); Salix*: Salix spp*. Error bars denote ±1 standard error. Crosses represent the values of the mean biomass. The actual data, including the numbers of observations, are listed in Supplementary Table 2.

https://doi.org/10.1038/s41477-024-01850-5

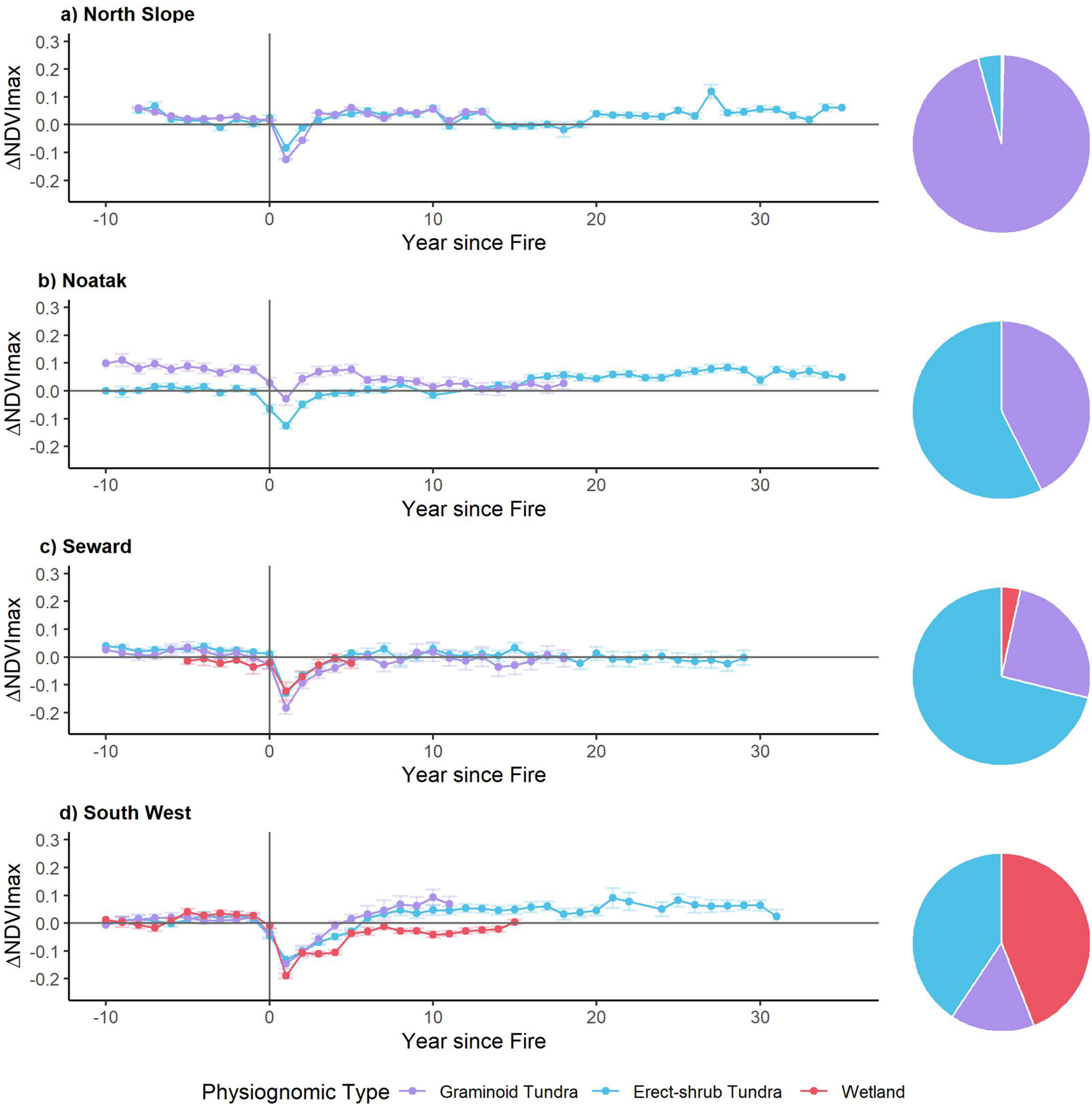

Extended Data Fig. 6 | Post-fire $NDVI_{max}$ anomaly trajectories for different physiognomic types and for high severity level burned points. Post-fire $NDVI_{max}$ anomaly trajectories for different physiognomic types (according to the 1 km CAVM raster dataset[44]) and for high severity level burned points. **a**–**d**, Tundra subregions North Slope (**a**), Noatak (**b**), Seward (**c**) and Southwest (**d**). Error bars denote ±1 standard error. The pie charts on the right show the relative proportions of the different physiognomic types among all high severity burned points in the corresponding subregion. The actual data, including the numbers of observations, are listed in Supplementary Table 3 (the trajectories) and Supplementary Table 4 (the pie charts), respectively.

 https://doi.org/10.1038/s41477-024-01850-5

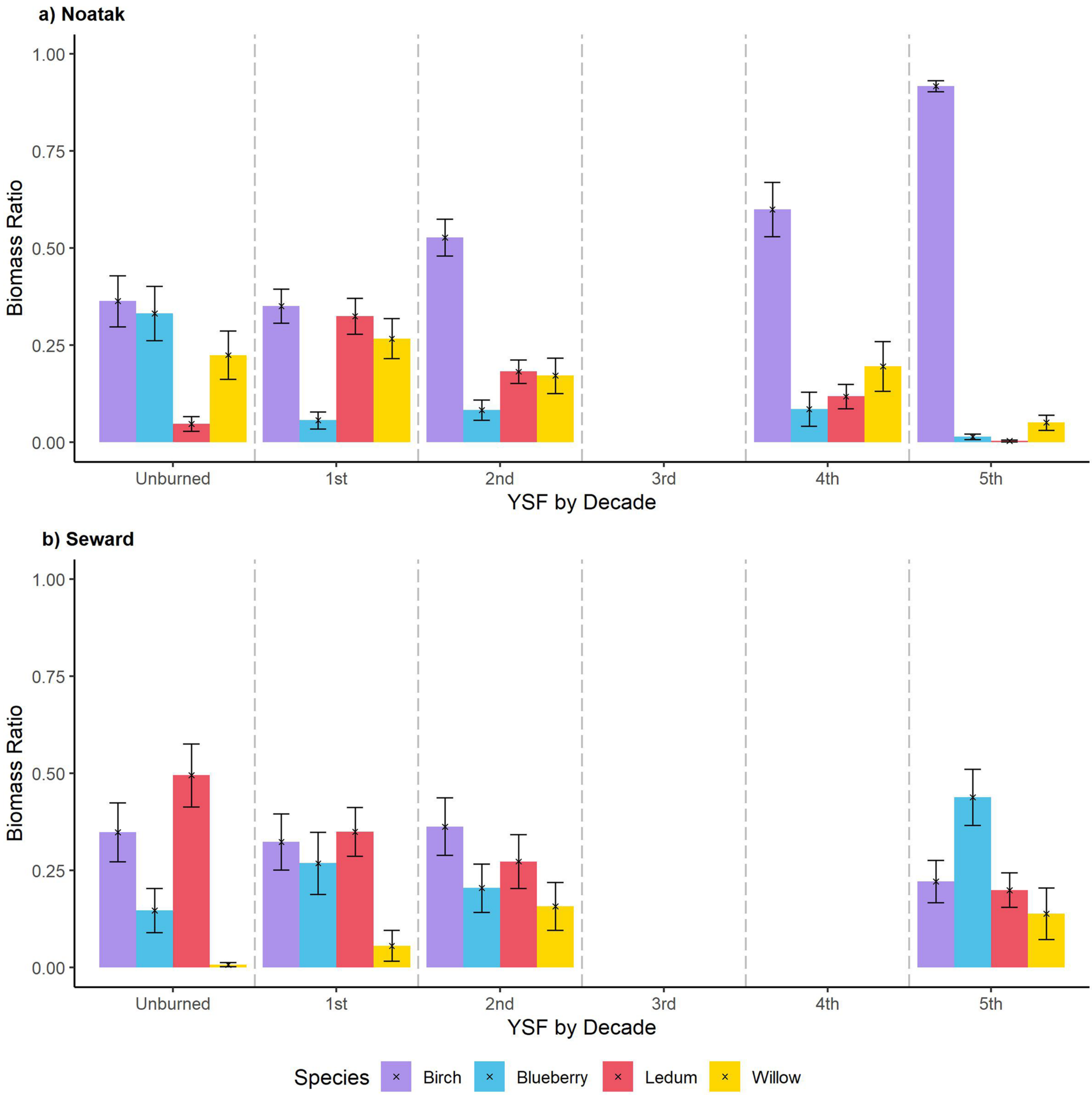

Extended Data Fig. 7 | Proportions of mean total biomass of four dominant shrub species for each stand age group calculated based on 1 x 1m plots in Noatak (a) and Seward (b). YSF: year since fire. Birch: *Betula nana;* Blueberry*: Vaccinium uliginosum;* Ledum*: Rhododendron groenlandicum* (bog Labrador tea); Willow*: Salix spp*. Error bars denote ±1 standard error. Crosses represent the values of the mean biomass. The actual data, including the numbers of observations, are listed in Supplementary Table 5.

 https://doi.org/10.1038/s41477-024-01850-5

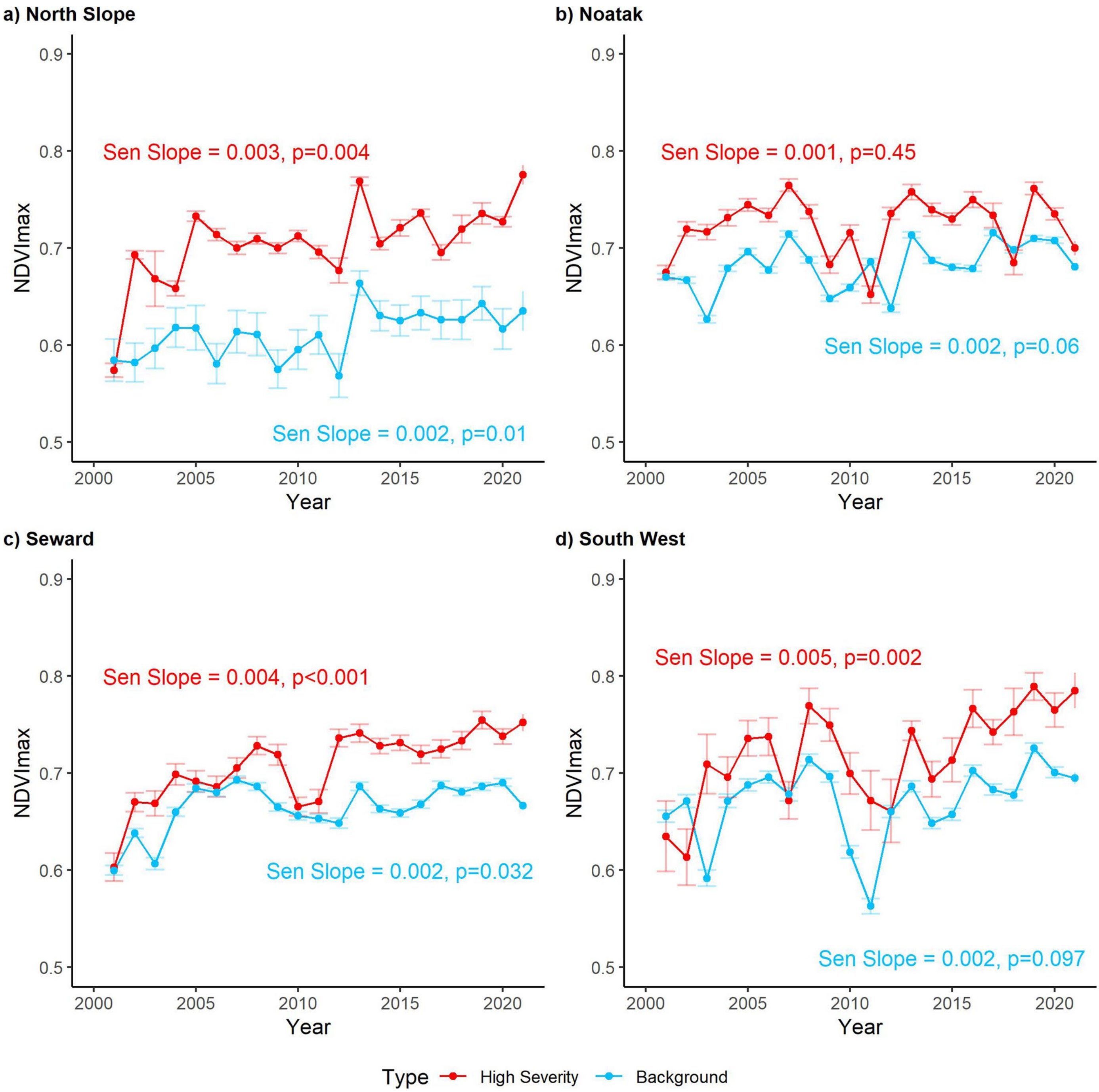

Extended Data Fig. 8 | NDVI$_{max}$ trajectories between 2001 and 2021 based on matching burned and background sample points. a–d, Panels correspond to tundra subregions North Slope (**a**), Noatak (**b**), Seward (**c**) and Southwest (**d**). Error bars denote ±1 standard error. The actual data, including the numbers of observations, are listed in Supplementary Table 6.

nature research

Corresponding author(s): Dong Chen

Last updated by author(s): Oct 8, 2024

Reporting Summary

Nature Research wishes to improve the reproducibility of the work that we publish. This form provides structure for consistency and transparency in reporting. For further information on Nature Research policies, see our Editorial Policies and the Editorial Policy Checklist.

Statistics

For all statistical analyses, confirm that the following items are present in the figure legend, table legend, main text, or Methods section.

n/a	Confirmed	
☐	☒	The exact sample size (*n*) for each experimental group/condition, given as a discrete number and unit of measurement
☐	☒	A statement on whether measurements were taken from distinct samples or whether the same sample was measured repeatedly
☐	☒	The statistical test(s) used AND whether they are one- or two-sided *Only common tests should be described solely by name; describe more complex techniques in the Methods section.*
☐	☒	A description of all covariates tested
☐	☒	A description of any assumptions or corrections, such as tests of normality and adjustment for multiple comparisons
☐	☒	A full description of the statistical parameters including central tendency (e.g. means) or other basic estimates (e.g. regression coefficient) AND variation (e.g. standard deviation) or associated estimates of uncertainty (e.g. confidence intervals)
☐	☒	For null hypothesis testing, the test statistic (e.g. *F*, *t*, *r*) with confidence intervals, effect sizes, degrees of freedom and *P* value noted *Give P values as exact values whenever suitable.*
☒	☐	For Bayesian analysis, information on the choice of priors and Markov chain Monte Carlo settings
☒	☐	For hierarchical and complex designs, identification of the appropriate level for tests and full reporting of outcomes
☒	☐	Estimates of effect sizes (e.g. Cohen's *d*, Pearson's *r*), indicating how they were calculated

Our web collection on statistics for biologists contains articles on many of the points above.

Software and code

Policy information about availability of computer code

Data collection	No software was used during data collection.
Data analysis	The following software/programing language were used: 1) ArcGIS Desktop 10.6; 2) Python 2.7.14; 3) IDL 8.5; 4) R 3.5.1; 6) Google Earth Engine (https://earthengine.google.com/). The LandsatTS package for R is available at https://github.com/logan-berner/LandsatTS.

For manuscripts utilizing custom algorithms or software that are central to the research but not yet described in published literature, software must be made available to editors and reviewers. We strongly encourage code deposition in a community repository (e.g. GitHub). See the Nature Research guidelines for submitting code & software for further information.

Data

Policy information about availability of data

All manuscripts must include a data availability statement. This statement should provide the following information, where applicable:
- Accession codes, unique identifiers, or web links for publicly available datasets
- A list of figures that have associated raw data
- A description of any restrictions on data availability

All data used in this paper are publicly accessible. The field data that our team collected is available through the Oak Ridge National Laboratory Distributed Active Archive Center (ORNL DAAC): https://doi.org/10.3334/ORNLDAAC/1919. The Alaska Vegetation Plots Database (AKVEG) is available at https://akveg.uaa.alaska.edu/. The Monitoring Trends in Burn Severity (MTBS) product is available at https://www.mtbs.gov/. The Circumpolar Arctic Vegetation Map (CAVM) dataset is available at https://www.geobotany.uaf.edu/cavm/.

Field-specific reporting

Please select the one below that is the best fit for your research. If you are not sure, read the appropriate sections before making your selection.

☐ Life sciences ☐ Behavioural & social sciences ☒ Ecological, evolutionary & environmental sciences

For a reference copy of the document with all sections, see nature.com/documents/nr-reporting-summary-flat.pdf

Ecological, evolutionary & environmental sciences study design

All studies must disclose on these points even when the disclosure is negative.

Study description	This study has two main analytical components: 1) extraction of NDVImax anomaly trajectories, and 2) analysis of field data. For the first component, we extracted annual NDVImax values at randomly generated sample points based on all available Landsat imagery hosted on Google Earth Engine. Our sample points are scattered across the Alaskan tundra, with 20,000 points generated for burned areas, 20,000 points generated for unburned areas, and 20,000 points generated for background unburned areas. For the second component, we analyzed the field data that were relevant to shrubs and established the relationship between shrub presence and a series of parameters, such as year since the last fire.
Research sample	For our analysis that was based on Google Earth Engine, a total of 60,000 sample points were generated across the Alaskan tundra. For the analysis that was based on field data, our analysis was based on data collected in 137 field sites in the Noatak River Valley (83 burned + 22 unburned) and the Seward Peninsula (21 burned + 11 unburned).
Sampling strategy	The sample points that were used in our Google Earth Engine-based analysis were randomly generated based on the wildfire history (Monitoring Trends in Burn Severity wildfire perimeters). In addition to the sample points for burned areas, we also generated the same amount of sample points for unburned areas, and they were generated randomly outside wildfire perimeters (within a buffer zone between 50 m and 1,000 m surrounding each fire perimeter). An additional group of background sample points were generated across the tundra that is below 300 m above sea level. The field sites where we collected field data were determined prior to our field trips based on a stratified randomized scheme taking into account a combination of factors including drainage, year since the last fire, and burn severity.
Data collection	At each site, the field team conducted measurements for a series of vegetation-related parameters at two different scales. We established one 1-m x 1-m plot within which we counted the number of shrub species as well as the number of stems of each species. We also estimated the biomass of the shrubs found within the 1-m × 1-m plot by applying the allometric equations which relate basal diameters to biomass. In addition, mean shrub height and percent shrub cover were measured and estimated, respectively. The majority of the measurements that are relevant to our manuscript were done by Tatiana Loboda and Liza Jenkins.
Timing and spatial scale	We collected field data in the tundra regions in Alaska between July and August in 2016, 2017, and 2018. Each field trip lasted for 1-2 weeks.
Data exclusions	Our field data contain parameters that are irrelevant to the current manuscript. Those data were excluded from the analysis of this manuscript.
Reproducibility	The technical procedures of this manuscript are well documented in order to facilitate the reproduction of the results.
Randomization	The sample points that were used in our Google Earth Engine-based analysis were randomly generated based on the wildfire history (Monitoring Trends in Burn Severity wildfire perimeters). In addition to the sample points for burned areas, we also had the same amount of sample points for unburned areas, and they were generated randomly outside wildfire perimeters (within a buffer zone between 50 m and 1,000 m). Background sample points were randomly generated across tundra areas that are below 300 m above sea level. The field sites where we collected field data were determined prior to our field trips based on a stratified randomized scheme taking into account a combination of factors including drainage, year since the last fire, and burn severity.
Blinding	The members who collected the field data that are relevant to shrubs (i.e., Tatiana Loboda and Liza Jenkins) were not involved in the data analysis process. In addition, the person who extracted NDVImax trajectories based on Google Earth Engine, Cheng Fu, had no prior knowledge about the intent of our analysis.

Did the study involve field work? ☒ Yes ☐ No

Field work, collection and transport

Field conditions	All our field work were conducted between July and August of 2016-2018, in the tundra regions in Alaska. We experienced a great variety of weather conditions during field data collection.
Location	In 2016 and 2018, our field sites were located in the Noatak River Valley in Alaska. In 2017, our field sites were in the Seward Peninsula, Alaska.
Access & import/export	During the two field trips to the Noatak River Valley, we entered and left the field sites via two single-engine fixed-wing planes. During the field trip to the Seward Peninsula, we entered and left the field sites via an SUV. Our field measurements were strictly abided by the local laws and regulations in Alaska. We obtained a permit (#NOAT-2016-SCI-0001) from National Park Service in 2016

	(renewed in 2018) for our field work in the Noatak River Valley. We obtained a permit (#LAS 31669) from the State of Alaska Department of Natural Resources in 2018 for our field work in the Seward Peninsula.
Disturbance	At each site, a hole no larger than 30cm x 30cm was dug to allow us to measure active layer depth and depth to mineral soil. The soils that were dug out were returned to the original hole once the measurement was completed.

Reporting for specific materials, systems and methods

We require information from authors about some types of materials, experimental systems and methods used in many studies. Here, indicate whether each material, system or method listed is relevant to your study. If you are not sure if a list item applies to your research, read the appropriate section before selecting a response.

Materials & experimental systems

n/a	Involved in the study
☒	☐ Antibodies
☒	☐ Eukaryotic cell lines
☒	☐ Palaeontology and archaeology
☒	☐ Animals and other organisms
☒	☐ Human research participants
☒	☐ Clinical data
☒	☐ Dual use research of concern

Methods

n/a	Involved in the study
☒	☐ ChIP-seq
☒	☐ Flow cytometry
☒	☐ MRI-based neuroimaging